Organization of Oriented Lamellar Structures in a Miscible Crystalline/Crystalline Polymer Blend under Uniaxial Compression Flow near the Melting Temperature

Akira Kaito,* Yuko Iwakura, Kohji Hatakeyama, and Yongjin Li

Nanotechnology Research Institute, National Institute of Advanced Industrial Science and Technology (AIST), Tsukuba 305-8565, Japan

Received December 25, 2006; Revised Manuscript Received February 5, 2007

ABSTRACT: Oriented lamellar structures were developed in a blend of poly(1,4-butylene succinate) (PBSU) and poly(vinylidene fluoride) (PVDF), a miscible crystalline/crystalline polymer blend, by uniaxial compression flow using a pair of channel plates. The temperatures of the compression flow were varied in the range 140−163 °C, at which PBSU was completely melted and PVDF was partially melted. Small-angle X-ray scattering (SAXS) and transmission electron microscopy (TEM) were used to analyze the lamellar morphologies, whereas the crystal orientation of PVDF and PBSU was determined by wide-angle X-ray diffraction (WAXD). The lamellar structure was highly oriented irrespective of processing conditions, but its morphology markedly depended upon the processing temperature. The lamellar stacks of the two polymers were mutually excluded from the interlamellar region (interlamellar exclusion), when the blended film was compression-processed below 150 °C. On the other hand, the lamellae of the two polymers were mutually included in the interlamellar regions, forming an alternately stacked lamellar sequence (interlamellar inclusion), when the processing temperature was higher than 150 °C. The interlamellar inclusion and interlamellar exclusion phenomena were explained by the formation and relaxation of the tie molecules between the lamellae. The crystal orientation of PBSU crystals was closely correlated with the lamellar morphologies. The WAXD results indicated that the crystal *b*-axis of PBSU was oriented parallel to the flow direction for the interlamellar exclusion structure and that the crystal *c*-axis of PBSU was preferentially oriented in the flow direction for the interlamellar inclusion structure. The oriented crystallization of PBSU was explained by the confined crystal growth of PBSU, which forces the fastest growth axis of PBSU crystals to align parallel to the ribbonlike domains of the interlamellar exclusion structure and in the lamellar plane of the interlamellar inclusion structure.

Introduction

Structure control of polymer blends has received considerable attention from the scientific point of view because a variety of factors are concerned with the structural organization. The phase morphologies and interfacial structures are important for immiscible polymer blends, whereas crystalline morphologies are essential for the physical properties of miscible polymer blends containing crystalline polymers. The lamellar structures and spherulitic morphologies in miscible crystalline polymer blends have been extensively studied by small-angle X-ray scattering (SAXS) and microscopic observations, respectively. The inclusion or exclusion of one component between the lamellae of another component is one of the important subjects in the former,[1−8] whereas the interpenetration of spherulitic growth is the major interest in the latter.[9−11] The interlamellar inclusion phenomenon was first evidenced for some miscible crystalline/amorphous polymer blends, such as poly(ϵ-caprolactone) (PCL)/poly(vinyl chloride) (PVC),[1] poly(ethylene oxide) (PEO)/poly(vinyl acetate),[2] and PEO/poly(methyl methacrylate),[3] from the increase in the long periods of lamellar stacks as the content of the amorphous component increases. More recently, the interlamellar inclusion and interlamellar exclusion structures have been extensively studied for miscible polymer blends containing two crystalline polymers. If the lamellae of a component with a higher crystallization temperature, T_c, include molecular chains of a lower T_c component, the crystallization of the lower T_c component results in the formation of an interlamellar inclusion structure. On the other hand, lamellar crystals of the two components in the blends are sometimes excluded from the interlamellar region during crystallization and independently constitute their own lamellar stacks. The lamellar structures of miscible crystalline/crystalline polymer blends are affected by composition and crystallization conditions. It was reported for the PCL/polycarbonate (PC) blends that PCL was rejected from the interlamellar region of PC in PCL-rich blends, whereas PCL was incorporated between the crystalline lamellae of PC in PC-rich blends.[4] In the case of poly(vinylidene fluoride) (PVDF)/poly(1,4-butylene adipate) (PBA) blends, there is a transition from interlamellar inclusion to interlamellar exclusion with an increase in the PBA content.[5,6] It was also found that the amounts of the interlamellar inclusion structures depend upon the crystallization condition of the PVDF/PBA blends.[6] Interlamellar inclusion structures have also been found for PVDF/poly(3-hydroxybutyrate) (PHB)[7] and PEO/poly(1,4-butylene succinate) (PBSU).[8]

The orientation control of polymer chains in miscible polymer blends has been extensively studied in past decades, aiming at inducing orientation textures that cannot be developed in single-component polymeric materials. Unique orientation textures have been induced by oriented crystallization in some miscible crystalline/amorphous polymer blends, such as PCL/PVC,[12,13] isotactic polystyrene (iPS)/poly(phenylene oxide) (PPO),[14] and poly[(*R*)-3-hydroxybutyrate] (PHB)/cellulose propionate (CP).[15] The crystallization of PCL in miscible blends with PVC under strain leads to crystalline orientation perpendicular to the strain direction under most conditions.[12,13] The oriented crystallization of iPS in oriented iPS/PPO blends results in an orientation

* Corresponding author: Tel +81-298-61-4443; fax +81-298-4437, e-mail a-kaito@aist.go.jp.

10.1021/ma062952g CCC: $37.00
Published on Web 03/22/2007

texture containing highly oriented iPS crystals and nearly isotropic PPO chains.[14] An orthogonal orientation texture has been developed by the oriented crystallization of PHB in PHB/CP blends in the CP-rich composition range.[15] Oriented crystallization has been also applied to the crystal orientation control of miscible crystalline/crystalline polymer blends, such as PBSU/PVDF blends[16] and PVDF/PHB blends.[17] For example, orthogonal orientation textures, in which the chain axes in crystals of the two components orient in mutually opposite directions, were induced by the oriented crystallization of PBSU in drawn films of PBSU/PVDF = 30/70 blends at slow crystallization rates.[16] Orthogonal orientation textures are also formed by the oriented crystallization of PHB in PVDF/PHB blends in the PVDF-rich composition range.[17] The mechanism of oriented crystallization was interpreted as a result of confined crystal growth that proceeds along the fibrillar axis in interfibrillar regions.[16] Only the interlamellar exclusion structure exists in drawn samples of the blends, and the orientation of the interlamellar inclusion structure has never been achieved yet. This is because the tie molecules formed by the drawing process might reject another component from the interlamellar region.

This work aims at producing new orientation textures with unique lamellar structures and crystal orientation in miscible crystalline/crystalline polymer blends. Oriented lamellar structures with interlamellar inclusion and those with interlamellar exclusion were formed in miscible crystalline polymer blends by uniaxial compression flow in the partially molten state. The blends studied in this work are miscible blends of poly(1,4-butylene succinate) (PBSU) (T_m = 112 °C) and poly(vinylidene fluoride) (PVDF) (T_m = 162 °C), whose miscibility and crystallization behaviors have been reported by Lee et al., in detail.[18] The PBSU/PVDF blend is an interesting polymer blend because the film of the blend can be easily stretched by external stress or flow, leading to the formation of unique lamellar structures with controlled crystal orientation. The improvement of the mechanical properties in two directions can be expected in relation to the structure organization.

Experimental Section

Materials and Sample Preparation. The PBSU and PVDF samples used in this work were purchased from Aldrich Chemical Co. Inc. and Scientific Polymer Products Inc., respectively. The molecular weight and polydispersity of the PBSU sample, determined by gel permeation chromatography, are M_w = 89 000 and M_w/M_n = 1.8, respectively. Those for the PVDF samples are M_w = 504 000 and M_w/M_n = 13.6, respectively. The PBSU/PVDF blends with a weight ratio of PBSU/PVDF = 30/70 were prepared by mixing the two polymers in an *N*,*N*-dimethylformamide (DMF) solution with a concentration of 3%. The blend samples were dried at 100 °C under vacuum for 2 days to remove the solvent. The blends were then hot-pressed at 185 °C to a sheet with a thickness of 800 μm, followed by rapid quenching in ice water.

Oriented samples were prepared under uniaxial compression flow for 20 min at a pressure of 100 MPa using a pair of channel plates, a sketch of which is shown in Figure 1a together with the principal axis, i.e., the flow direction (FD), the width direction (WD), and the normal direction (ND) to the sheet plane. The samples, which were set in the channel of the plates, flowed or deformed along the channel of the plates under shear and extensional strains during compression processing. The processing temperatures were varied in the range 140−163 °C, at which PBSU was completely melted and PVDF was partially melted. The temperature of the plates was calibrated by observing the melting of indium, which was placed in the channel of the lower plate. The pressed samples were quenched in ice water together with the die, immediately after the load release. The oriented samples obtained under compression flow are designated to be "flow-oriented samples". The draw ratio was determined from the ratio of lengths before and after compression processing. The draw ratio increases stepwise by raising the processing temperature, as shown in Figure 1b.

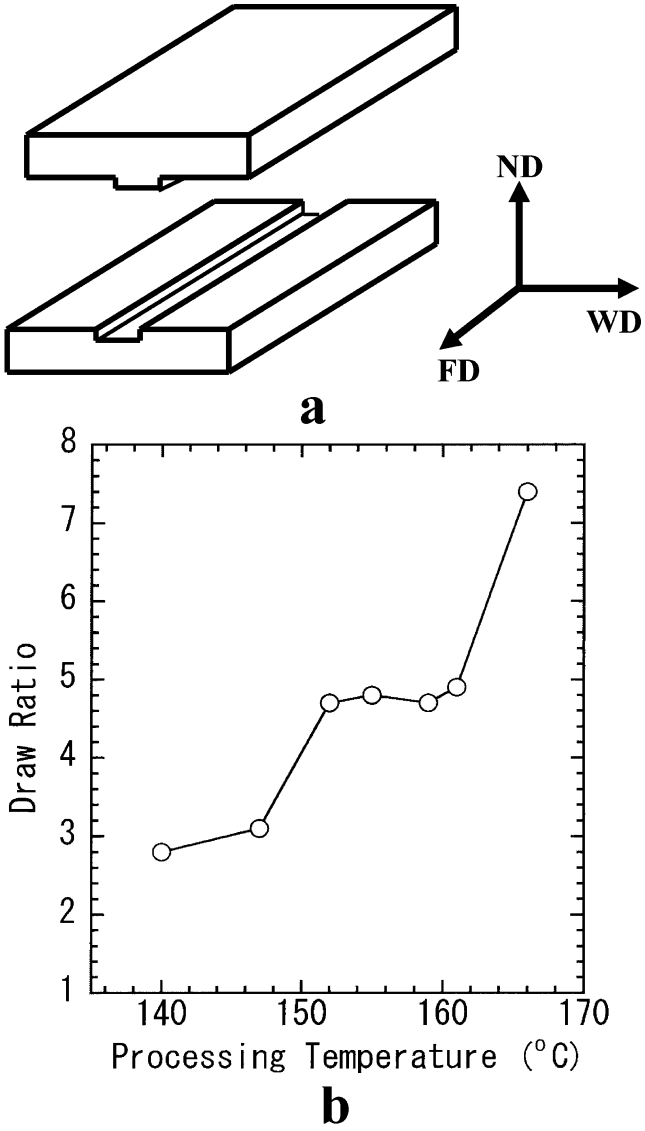

Figure 1. (a) Sketch of a pair of channel plates together with the principal axis, i.e., the flow direction (FD), the width direction (WD), and the normal direction (ND) to the sheet plane. (b) Draw ratio vs processing temperature.

Characterization. Differential scanning calorimetry (DSC) measurements were carried out under nitrogen flow at a heating rate of 10 °C/min with a Perkin-Elmer DSC-7 differential scanning calorimeter calibrated with the melting temperatures of indium and zinc.

The two-dimensional SAXS images were measured with fine-focused Cu Kα radiation (45 kV, 60 mA) generated by an X-ray diffractometer, Rigaku, Ultrax 4153A 172B. A scattering angle resolution of $2\theta = 0.09°$ was achieved with a pair of beam-focusing mirrors, confocal MAX flux optics, and three collimation slits. The SAXS images were detected with an imaging plate detector, Rigaku RAXIS-DS3C. The SAXS profiles were also obtained directly from the imaging plates.

The WAXD measurements were conducted using Cu Kα radiation (40 kV, 120 mA) with a wavelength of 0.1542 nm generated by an X-ray diffractometer, Rigaku Ultrax 18SF. The WAXD images and the equatorial and meridional profiles were obtained with an imaging plate, Rigaku RAXIS-DS3C.

Transmission electron microscopy (TEM) images of the oriented blends were obtained at an acceleration voltage of 75 kV using an

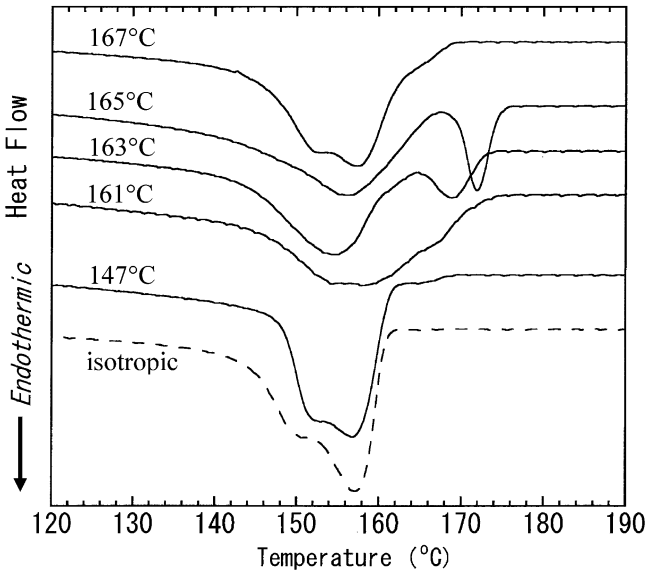

Figure 2. DSC curves of PBSU/PVDF = 30/70 blends flow-oriented at various temperatures together with a DSC curve of an isotropic blend.

H7000 (Hitachi) transmission electron microscope. The oriented samples were embedded in an epoxy resin, and its microtomed surface was stained with RuO_4 vapor for 24 h. The samples were microtomed into thin sections 70 nm in thickness parallel to the flow direction at a rate of 1 mm/s. The sections collected into a 200 mesh copper grid were served for the TEM measurement.

Rectangle-shaped specimens 3 mm in width and 25 mm in length were cut from the oriented films in two directions and were used for tensile tests, which were carried out both in the flow direction and in the direction perpendicular to it at a tensile rate of 2 mm/min, at 20 °C and 50% relative humidity, using a tensile testing machine, Tensilon UMT-300 (Orientec Co. Ltd.). The tear strength of samples was also measured using the tensile testing machine and a specially designed apparatus. Samples 5 mm in width and 30 mm in length were fixed at the bottom of the tensile testing machine, and a knife with an edge angle of 30° was attached to the lower part of a load cell that was fixed on the crosshead of the tensile testing machine. The sample was torn parallel to the flow direction by lowering the knife at a rate of 20 mm/min together with the crosshead of the tensile testing machine. The tear strength was obtained by dividing the tearing load by the thickness of the samples.

Results

Thermal Behaviors. Figure 2 shows the DSC curves of the PBSU/PVDF = 30/70 blends flow-oriented at various temperatures and that of the isotropic blend in the temperature range of the melting of PVDF. The DSC curves were normalized by sample weight after a baseline correction. The DSC curve of the sample flow-oriented at 147 °C is similar to that for the isotropic sample as a whole but shows a small shoulder around 165 °C. The shoulder is intensified and spread over the higher temperature region for the sample flow-oriented at 161 °C. A clear endothermic peak is observed at 169 °C in addition to the main peak around 155 °C for the sample flow-oriented at 163 °C. The high-temperature peak is intensified and shifts to a higher temperature as the processing temperature is raised. These results indicate that the oriented crystals with thick lamellae are formed during compression processing and that the amount and the lamellar thickness increase by raising the processing temperature. The high-temperature peak, however, decreases for the sample flow-oriented at 167 °C.

Lamellar Structures. Figure 3 shows schematic illustrations for the oriented lamellar morphologies and their expected SAXS images. The molecular chains of a component with a lower crystallization temperature (T_c) are sometimes excluded from the lamellar stacks of a component with a higher T_c, forming their own lamellar stacks in blends (interlamellar exclusion structure), as shown in Figure 3a. On the other hand, if the lamellae of a component with a higher T_c include amorphous chains of a lower T_c component, the interlamellar inclusion structure is induced by the crystallization of a component having a lower T_c (Figure 3b). The two lamellar structures can be identified by SAXS when the difference in the density between the components is larger than the density difference between the crystalline and amorphous phases in each component in the blend. The densities of PVDF and PBSU are 1.78 and 1.23 g/cm^3, respectively. The PBSU/PVDF blends are suitable for the SAXS analysis because of the large density difference. An SAXS peak originating from the density difference of the components is expected in the low-angle range for the interlamellar inclusion structure because the long period L is roughly the sum of the long periods for the components, L_1 and L_2. On the other hand, the long period for the interlamellar exclusion structure is the weighted average of L_1 and L_2. Intense scattering is expected in the equatorial direction for the interlamellar exclusion structure in addition to meridional scattering because a large electron density fluctuation is induced due to the periodic arrangement of the lamellar stacks perpendicular to the orientation direction. Thus, the two lamellar morphologies can be distinguished by the long period and the intensity pattern of the SAXS images.

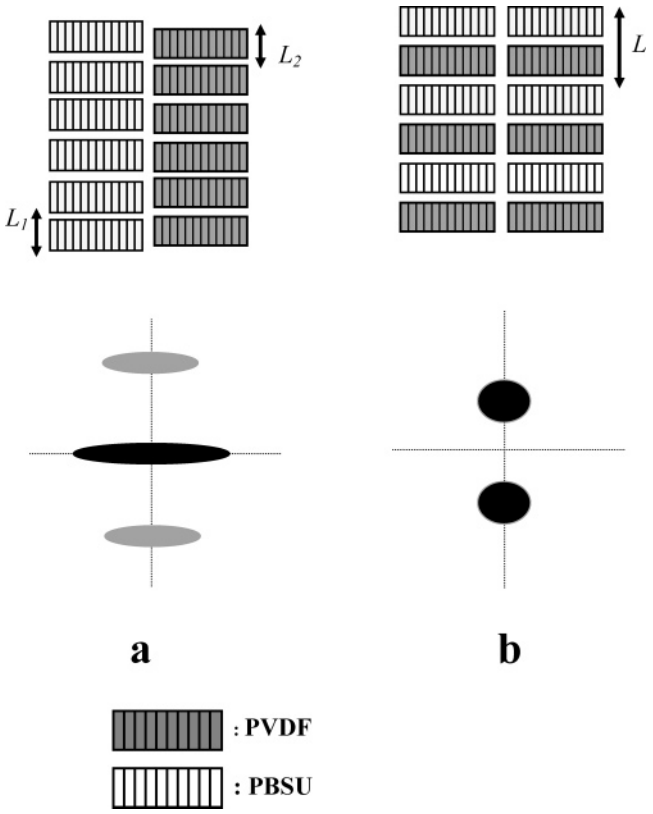

Figure 3. Schematic illustrations for oriented lamellar morphologies and their expected SAXS images: (a) interlamellar exclusion structure; (b) interlamellar inclusion structure.

Figure 4 shows the SAXS images for the PBSU/PVDF blends flow-oriented at various temperatures, which are presented at the same magnification. Figure 4a−e shows the SAXS images of the PBSU/PVDF = 30/70 blends flow-oriented at 140−163 °C, which were measured with an incident X-ray beam in the normal direction. The films flow-oriented at 140 and 147 °C

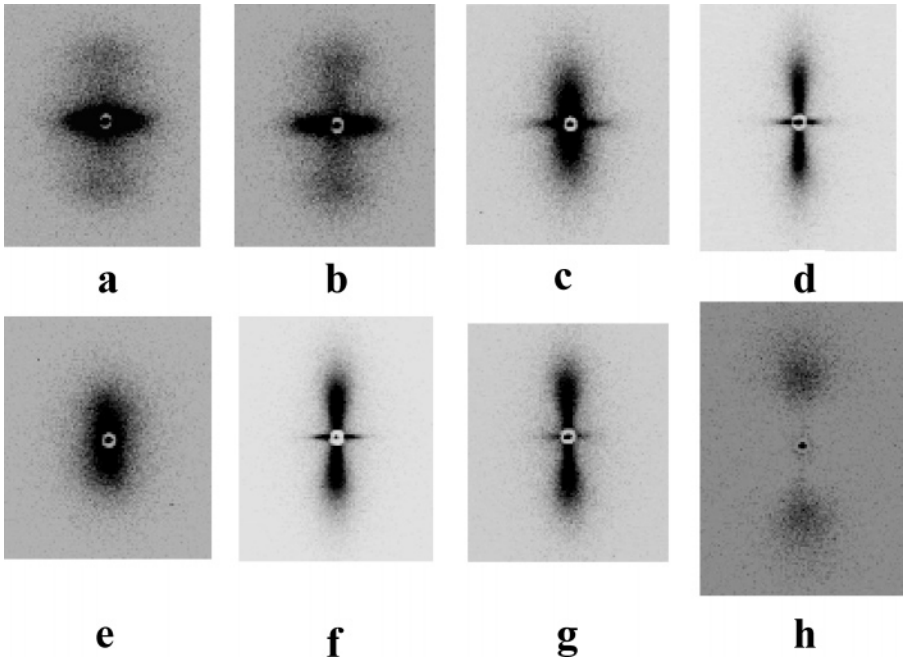

Figure 4. SAXS images of flow-oriented samples of PBSU/PVDF blends: (a) PBSU/PVDF = 30/70 blends flow-oriented at 140 °C, (b) PBSU/PVDF = 30/70 blends flow-oriented at 147 °C, (c) PBSU/PVDF = 30/70 blends flow-oriented at 155 °C, (d) PBSU/PVDF = 30/70 blends flow-oriented at 161 °C (normal direction), (e) PBSU/PVDF = 30/70 blends flow-oriented at 163 °C, (f) PBSU/PVDF = 30/70 blends flow-oriented at 161 °C (width direction), (g) PBSU/PVDF = 15/85 blends flow-oriented at 161 °C, (h) pure PVDF flow-oriented at 161 °C. The incident X-ray beam is normal to the film plane (ND) for the images of (a−e, g, h), whereas the incident X-ray beam is parallel to the width direction (WD) for the image of (f). Flow direction is vertical in all SAXS images.

exhibit strong equatorial scattering as well as meridional scattering, indicating the presence of the interlamellar exclusion structure in these samples (Figure 4a,b). The meridional scattering is intensified and shifts to a lower angle accompanied by a decrease in equatorial scattering for the film flow-oriented at 155 °C (Figure 4c). The lamellar structure is transformed from interlamellar exclusion to interlamellar inclusion by raising the processing temperature from 147 to 155 °C. The SAXS pattern of the film flow-oriented at 161 °C is characterized by a linelike scattering pattern that is elongated along the meridian (Figure 4d), indicating that the interlamellar inclusion structure is highly oriented in the flow direction in the sample. The degree of orientation for the sample seems higher than that of the film flow-oriented at 155 °C, although the processing temperature is close to the end-melting temperature of PVDF crystals. The highly oriented structure in the sample flow-oriented at 161 °C is stabilized by the oriented crystals with high melting temperature (T_m), which are induced during compression processing. The degree of orientation of the interlamellar inclusion structure becomes relaxed with further increasing the processing temperature, as shown in Figure 4e. Figure 4f shows the SAXS image of the PBSU/PVDF = 30/70 blend flow-oriented at 161 °C, which was measured with an incident X-ray beam along the width direction. The SAXS image in Figure 4f is very similar to that of the same sample measured from the normal direction (Figure 4d), indicating that the mode of the lamellar orientation is uniaxial in spite of the nonuniaxial processing procedure.

The composition dependence of the SAXS images of the sample flow-oriented at 161 °C can be seen from a comparison of parts d, g, and h of Figure 4. The figures show that the highly oriented lamellar structures are also induced in pure PVDF and the PBSU/PVDF = 15/85 blend by uniaxial compression flow. The meridional scattering shifts to a higher angle as the PBSU content decreases. The long periods obtained from the scattering peaks increase with an increase in the PBSU content (Table 1), suggesting the inclusion of PBSU crystals between the lamellae of PVDF. It is, however, difficult to prepare a highly oriented lamellar inclusion structure for PBSU/PVDF blends containing more than 40% PBSU because the interlamellar exclusion structure is dominant over the interlamellar inclusion structure for PBSU-rich blends.[19]

Table 1. Long Periods of PVDF, PBSU, and PBSU/PVDF Blends

sample	processing	long periods (nm)
PVDF	isotropic	9.4
PBSU	isotropic	8.8
PBSU/PVDF = 30/70	flow-oriented at 140 °C	12.2
PBSU/PVDF = 30/70	flow-oriented at 147 °C	12.8
PBSU/PVDF = 30/70	flow-oriented at 152 °C	17.5
PBSU/PVDF = 30/70	flow-oriented at 155 °C	18.5
PBSU/PVDF = 30/70	flow-oriented at 159 °C	15.7
PBSU/PVDF = 30/70	flow-oriented at 161 °C	17.5
PBSU/PVDF = 15/85	flow-oriented at 161 °C	16.5
PVDF	flow-oriented at 161 °C	10.6

Figure 5a shows the Lorentz-corrected meridional SAXS profiles of the PBSU/PVDF = 30/70 blends flow-oriented at various temperatures. The SAXS profiles of the melt-quenched films of pure PVDF and PBSU are shown in Figure 5b for comparison. The films flow-oriented below 150 °C contain excluded lamellar stacks of PVDF and PBSU as judged from the SAXS image, but the long periods of the films are longer than those of pure polymers (Table 1), indicating that some PBSU chains might be partially diffused into the interlamellar region of PVDF during compression processing at 140−147 °C. The peak of meridional SAXS shifts to a lower angle (q = 0.34−0.4 nm^{-1}) in the films flow-oriented at 152−161 °C owing to the formation of the interlamellar inclusion structure. The long periods of these samples lie in the range 15.7−18.5 nm and almost agree with the sum of the periods of pure PVDF and PBSU. The values of the long periods also support the formation of the oriented interlamellar inclusion structure in the samples.

Crystal Orientation. Parts a and b of Figure 6 show the WAXD images of the PBSU/PVDF = 30/70 blends flow-

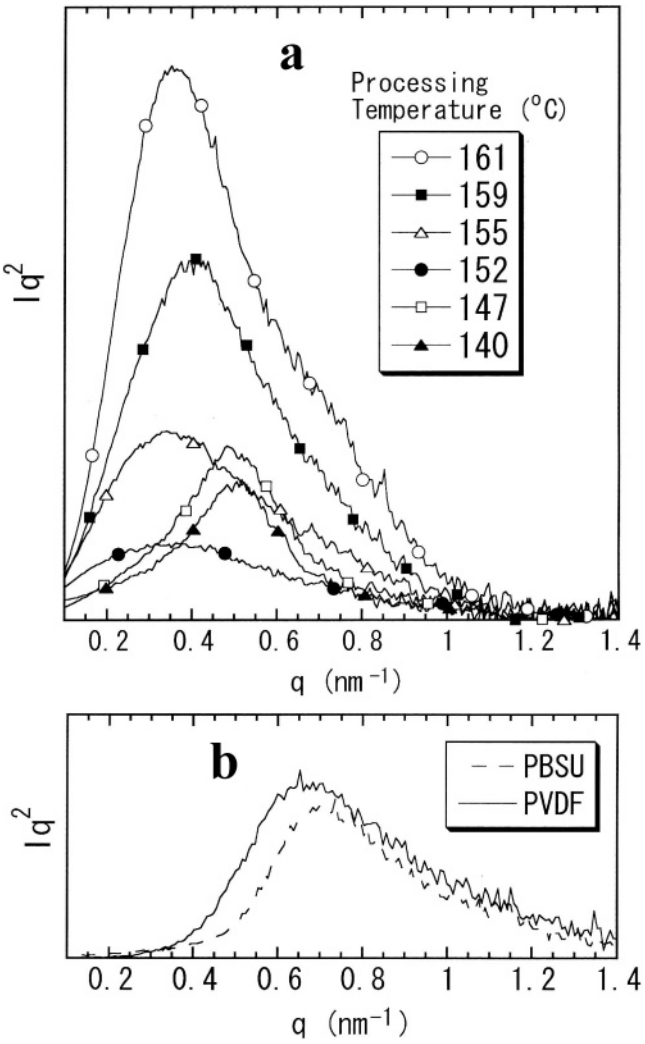

Figure 5. (a) Lorentz-corrected meridional SAXS profiles of PBSU/PVDF = 30/70 blends flow-oriented at various temperatures. (b) Lorentz-corrected SAXS profiles of melt-quenched samples of pure PBSU and PVDF.

oriented at 147 and 161 °C, respectively, which were measured with an incident X-ray beam in the normal direction. Figure 7 shows the equatorial and meridional WAXD profiles of the same samples, which were obtained from the WAXD images. The WAXD reflections of the α- and β-crystalline forms of PVDF are observed in Figures 6 and 7, indicating that the two crystalline forms of PVDF coexist in the oriented samples of the PBSU/PVDF blends. The former exhibits 100, 020, and 110 reflections at $2\theta = 17.9°$, 18.4°, and 20.1°, respectively, in the equatorial profiles of Figure 7a,b, whereas the latter shows 110 and 200 reflections at $2\theta = 20.8°$ in the equatorial direction. The content of the α-crystalline form increases and that of the β-form decreases with an increase in the processing temperature. The appearance of the *hk*0 reflections of PVDF crystals in the equatorial direction indicates that the crystal *c*-axis (molecular chain axis) of the two crystalline forms of PVDF is oriented in the flow direction for all samples. On the other hand, the crystal orientation of PBSU depends upon the lamellar morphologies. PBSU crystallizes in a monoclinic crystal lattice with the parameters $a = 0.523$ nm, $b = 0.908$ nm, $c = 1.079$ nm, and $\beta = 123.87°$.[20] The major reflections of PBSU are 020, 021, and 110 reflections, which are expected at $2\theta = 19.6°$, 21.2°, and 22.7°, respectively. The 020 reflection of PBSU is observed in the meridian, and the 021 reflection is located at 20°−25° from the meridian in the sample flow-oriented at 147 °C (Figure 6a). The 020 and 021 reflections are clearly observed in the meridional profile of the sample processed at 147 °C, whereas the *hk*0 reflections of the α- and β-forms of PVDF crystals dominate the equatorial profile (Figure 7a). The WAXD results indicate that the *b*-axis of PBSU crystals is oriented parallel to the flow direction and that the crystal *a*- and *c*-axes of PBSU are aligned perpendicular to the flow direction in the sample with the interlamellar exclusion structure. On the other hand, the 020 reflection of PBSU is observed in the equatorial direction of the WAXD image in the sample flow-oriented at 161 °C (Figure 6b), and the 020, 021, and 110 reflections are identified in the equatorial WAXD profile (Figure 7b), indicating that the crystal *c*-axis of PBSU is preferentially oriented in the flow direction for the sample having the interlamellar inclusion structure. The crystal orientation becomes relaxed by raising the processing temperature above 161 °C.

Morphologies. Figure 8a shows the TEM image of the PBSU/PVDF = 30/70 blend flow-oriented at 147 °C. It was reported that the crystalline polymers were selectively stained with RuO_4,[21] which makes it possible to observe the morphologies of blends of crystalline polymers. For example, polyolefins, polyesters, and polyamides are readily stained with RuO_4, but RuO_4 is not active on PVDF, poly(vinyl chloride), and polyacrylonitrile.[21] The bright and dark regions correspond to the PVDF-rich and PBSU-rich domains, respectively, because

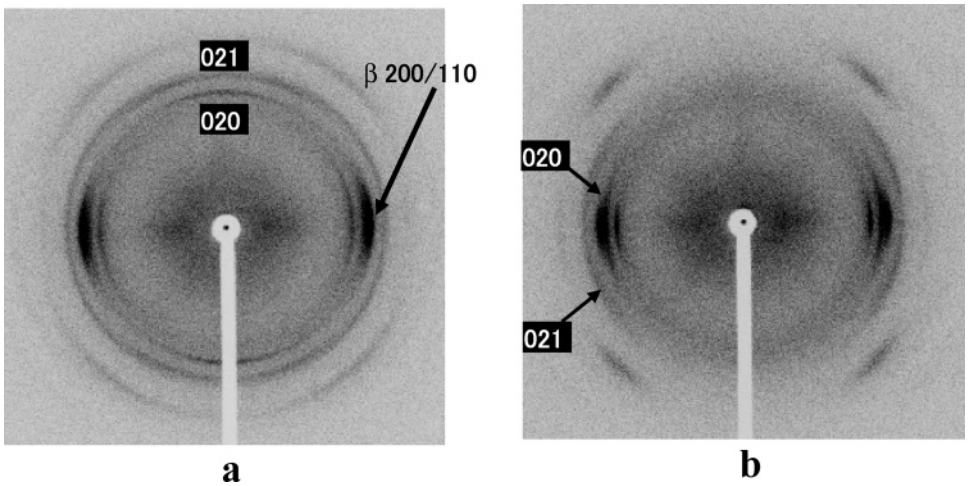

Figure 6. WAXD images of PBSU/PVDF = 30/70 blend flow-oriented at (a) 147 and (b) 161 °C. Flow direction is vertical in WAXD images. Black letters show the reflections of the α- and β-form crystals of PVDF, while the white letters show the reflections of PBSU.

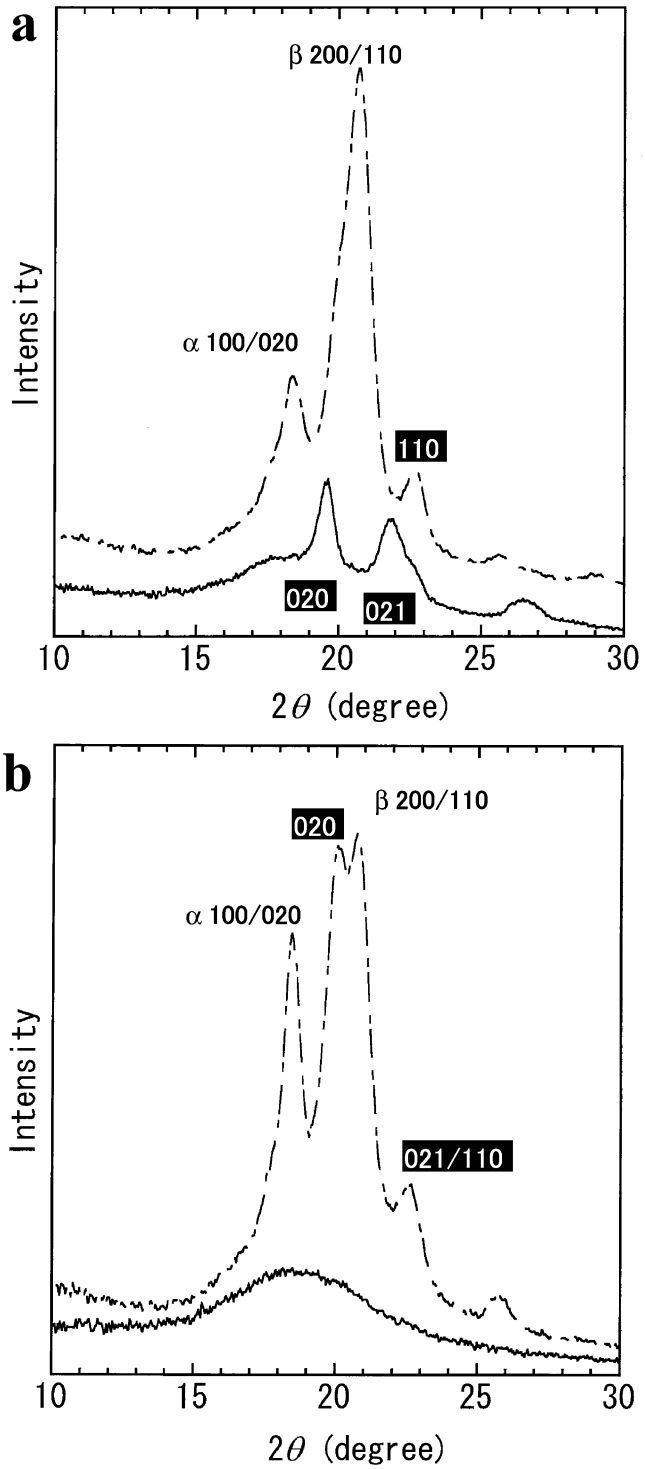

Figure 7. Meridional (solid line) and equatorial (chain line) WAXD profiles for PBSU/PVDF = 30/70 blend flow-oriented at (a) 147 °C and (b) 161 °C. Black letters show the reflections of the α- and β-form crystals of PVDF, while the white letters show the reflections of PBSU.

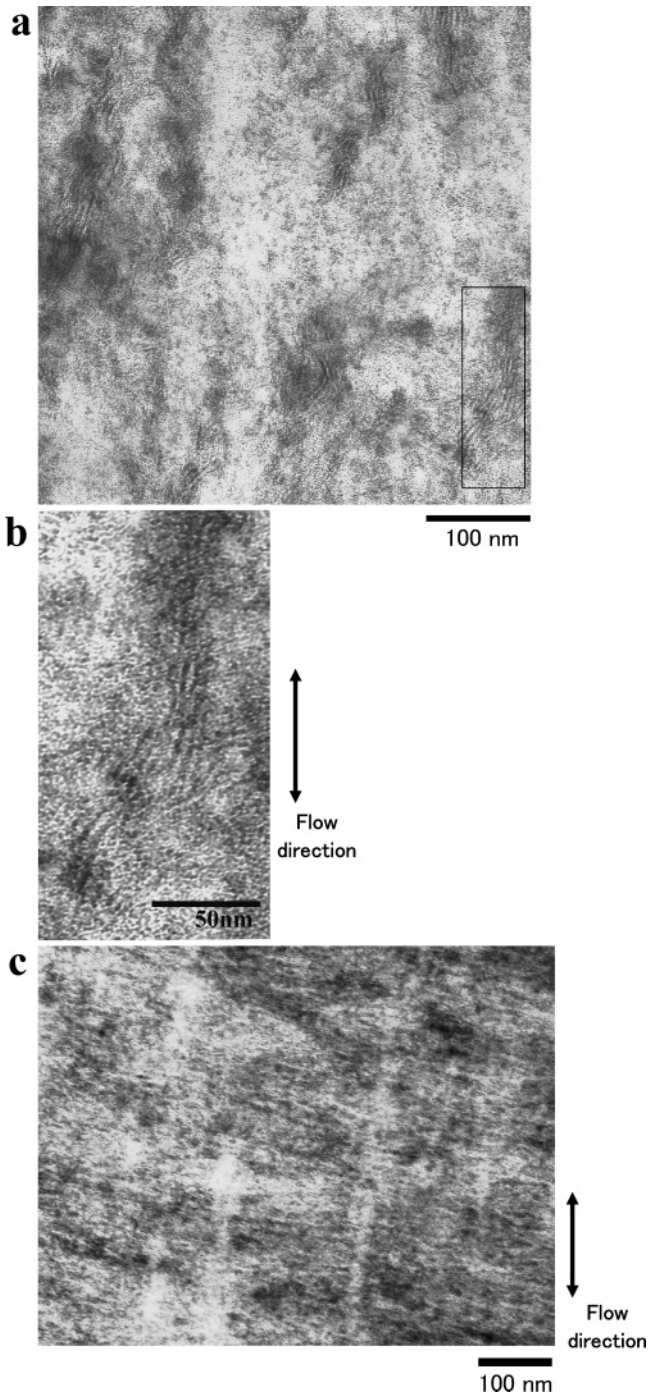

Figure 8. TEM images of the PBSU/PVDF = 30/70 blends: (a) flow-oriented at 147 °C, (b) flow-oriented at 147 °C, expansion of the enclosed part of (a), and (c) flow-oriented at 161 °C.

the PVDF-rich domains cannot be stained with RuO_4. The lamellae of PVDF are not identified in the TEM micrographs because the strained tie molecules, which are formed between PVDF lamellae during compression processing, disturb the diffusion of RuO_4. The PVDF-rich and PBSU-rich domains are elongated along the flow direction, forming ribbonlike domains with diameters of 50−100 nm. Figure 8b is an expansion of the enclosed part of Figure 8a, which consists of several lamellae of PBSU with a long period of 7−9 nm. The lamellar surface of PBSU crystals are oriented parallel to the flow direction, indicating the perpendicular orientation of the chain axis in the flow direction. The observed morphologies are in agreement with those expected from the results of SAXS and WAXD as a whole. Figure 8c shows the TEM image of the samples flow-oriented at 161 °C. The bright rodlike structures, which are oriented parallel to the flow direction, are interpreted as the high-T_m crystals of PVDF formed under uniaxial flow. Bright and dark lines are alternately running perpendicular to the rodlike structures and correspond to the lamellae of PVDF and PBSU, respectively, in the interlamellar inclusion structure. The long period observed in the TEM image is 15−25 nm and coincides with the value expected by SAXS.

Mechanical Properties. It is interesting to study the influence of the lamellar morphology and crystal orientation of PVDF

Table 2. Mechanical Properties of PBSU/PVDF = 30/70 Blends

processing	direction	yield strength (MPa)	breaking strength (MPa)	strain at break (%)	tear strength[b] (N/mm)
flow-oriented at 147 °C	||		106.4	78.6	1.8
flow-oriented at 147 °C	⊥	29.5	26.7	235.0	
flow-oriented at 155 °C	||		74.7	50.1	2.2
flow-oriented at 155 °C	⊥	32.1	27.5	210	
flow-oriented at 161 °C	||		63.7	60.2	2.4
flow-oriented at 161 °C	⊥	30.9	28.9	555	
as-drawn at 75 °C[a]	||		197.0	35.5	0.45
as-drawn at 75 °C[a]	⊥	22.5	20.5	452	
isotropic		25.0	25.7	697	1.9

[a] Reference 16. [b] Averaged over the strain range of 6−22 mm.

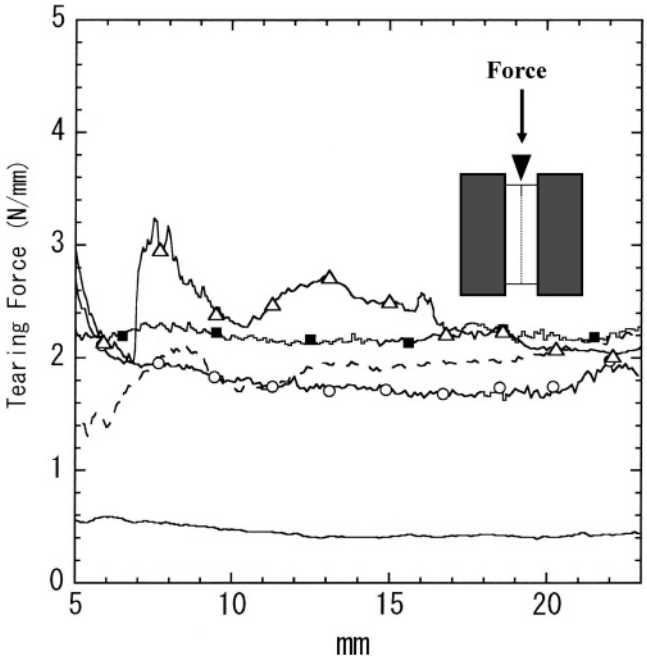

Figure 9. Tearing force vs distance curves of flow-oriented films of PBSU/PVDF = 30/70 blends, as well as a sketch of the tearing apparatus: (○) flow-oriented at 147 °C, (■) flow-oriented at 155 °C, (□) flow-oriented at 161 °C, (- - -) isotropic film, and (—) as-drawn film.

and PBSU on the mechanical properties of the material. The results of tensile tests for the flow-oriented blends are shown in Table 2 as well as those for an isotropic film and a uniaxially drawn film of the blends. A yield point is observed in the stress−strain curve of a flow-oriented sample when it is stretched perpendicular to the flow direction (width direction in Figure 1a), whereas a sample is deformed without yielding under stretching in the flow direction. The ultimate strengths of the flow-oriented samples in the flow direction are lower than the strength of the drawn sample in the drawing direction and decrease by raising the processing temperature. On the other hand, the flow-oriented samples shows 1.3−1.4 times higher yield strength in the perpendicular direction than the drawn sample. The yield strengths of the flow-oriented samples also exceed the strength of the isotropic blend film in both the flow and perpendicular directions.

Figure 9 shows the tearing force of the flow-oriented films, drawn film, and isotropic film of the blends as well as a sketch of the tearing apparatus. The tearing load is not stable in the initial stage (5−6 mm) of the tearing tests, in which the knife is entering the sample, but a plateau region appears in the load−distance curve in the tearing process. The tear strength, averaged in the plateau region of Figure 9, is also presented in Table 2. In general, the tear strength is markedly decreased in uniaxially oriented films with respect to isotropic films, owing to the formation of an oriented fibrillar structure. In fact, the tear strength of the drawn film is only 23% of the isotropic film for the PBSU/PVDF = 30/70 blend. The tear strengths of the flow-oriented blend films are, however, in the same range of tear strength as the isotropic blend film. The tear strength tends to increase with an increase in the processing temperature and exceeds the tear strength of the isotropic sample at higher processing temperatures (155−161 °C). Although the trouser tear method (ISO6383-1) is one of the most general tear testing methods, flow-oriented films cannot be torn by this method owing to the high tear strength. The sample flow-oriented at 147 °C favors the interlamellar exclusion structure, but the PBSU chains are partially incorporated between the lamellae of PVDF. Moreover, the crystal *b*-axis of PBSU is oriented in the flow direction, and thereby the crystal *c*-axis of PBSU will be aligned perpendicular to the flow direction. The crystal orientation and the diffusion of the PBSU chains in the interlamellar regions are concerned with the improvement of the vertical strength and the tear strength. On the other hand, the interlamellar inclusion structure in the sample flow-oriented at 161 °C also contributes to the improvement of the mechanical properties. The interlamellar inclusion structure forms continuous layers perpendicular to the flow direction, which suppress the crazing along the flow direction.

Discussion

Formation of Oriented Lamellar Morphologies. It is important to consider the mechanism of the formation of the oriented lamellar morphologies, which is markedly dependent on the processing temperature and the crystallinity of PVDF under compression flow. The structure organization under compression processing below 150 °C is similar to that for the oriented crystallization in the drawn PBSU/PVDF films, which was discussed in our previous paper.[16] The degree of crystallinity of PVDF is evaluated as being higher than 75% below 150 °C from the DSC curve of the blend. The crystallites of PVDF are rearranged into the fibrillar structure with the crystal *c*-axis along the flow direction. In addition, the tie molecules should be formed between the crystallites of PVDF and act as stress transmitters under compression flow. It is expected that the tie molecules would reject the PBSU chains from the lamellar stacks of PVDF. The PBSU chains might crystallize in the interfibrillar region during the cooling process for the sample flow-oriented below 150 °C. Figure 10 shows a model for the structure development under compression flow at 161 °C, where the crystallinity of PVDF almost disappears. The results of DSC suggest that the oriented crystals of PVDF with high T_m are induced during the structure organization at 161 °C. Structural development during melt-spinning of PVDF was studied using simultaneous in-situ synchrotron SAXS and WAXD.[22,23] It was reported that the shish crystals of PVDF were developed at the initial stage of spinning, followed by the formation of kebab crystals.[22,23] In the present case, the oriented crystals of PVDF

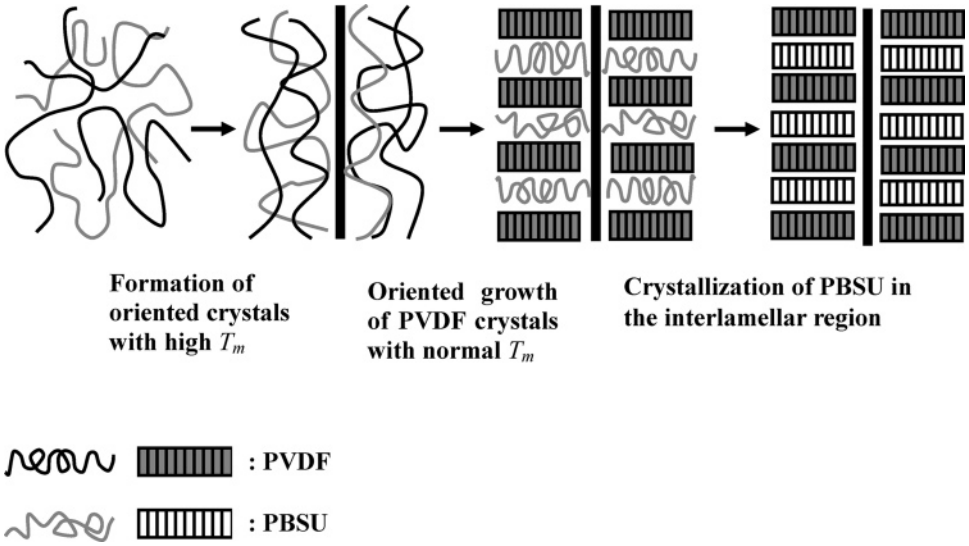

Figure 10. Schematic illustration for structure formation during compression processing above 150 °C.

with high T_m are induced in the initial stage of compression processing, and those with normal-T_m grow on the high-T_m crystals in the next step. Finally, the PBSU chains crystallize between the lamellae of PVDF, resulting in the formation of the interlamellar inclusion structure with a high degree of orientation. The mechanism of structure formation is complicated and not very clear under compression flow at intermediate temperatures (150−158 °C). Although the crystallinity of PVDF is much decreased in the intermediate temperature range, the crystallites of PVDF remain during compression processing. The PBSU chains tend to diffuse into the interlamellar region of PVDF because the tie molecules decrease and are relaxed in the intermediate temperature range. The meridional SAXS peak of the sample flow-oriented at 150 and 155 °C is broad and shifts to a lower scattering angle (longer period) with respect to the SAXS peak of the sample flow-oriented at 159−161 °C. In addition, the intensity of meridional SAXS is lower in the sample flow-oriented at 150−155 °C than in the sample at 159−161 °C. It is clear from the SAXS results that the interlamellar inclusion structure is stable in both cases, but the lamellar structure is less ordered for the samples flow-oriented at intermediate temperatures in degree of orientation and periodicity than that of the sample at 161 °C. The reason for the difference is not clear, but one possible explanation is that the inclusion of PBSU crystals between the lamellae of PVDF is irregular for the samples flow-oriented at intermediate temperatures.

The lamellar structures of PBSU/PVDF = 30/70 blends change from interlamellar exclusion into interlamellar inclusion as the processing temperature increases to around 150 °C. We have recently reported that the lamellar structure is transformed from interlamellar inclusion into interlamellar exclusion during the stretching of films of miscible crystalline/crystalline polymer blends.[16,17,19] These results suggest that the relaxation of the tie molecules controls the lamellar structures. The interlamellar exclusion structure is stable under compression flow below 150 °C because the tie molecules are formed between the lamellae of PVDF and transmit stress during compression processing. The tie molecules between PVDF crystals are relaxed, and their amount decreases by raising the processing temperature. The relaxation of the tie molecules makes mutual diffusion of the components possible, even in highly oriented samples.

Oriented Crystallization of PBSU in Confined Domains. The crystallization temperature of PBSU is lower than that of PVDF, which means that the crystallization of PBSU occurs in the preexisting morphology of PVDF. The crystal orientation of PBSU is induced by crystal growth in the morphology of PVDF. Up to now, epitaxial crystallization,[24−26] thermal shrinkage stress,[27] and transcrystallization[28−30] have been used to interpret some new crystalline textures formed in some other blends. The possibility of an epitaxial crystallization of PBSU on the surface of PVDF is ruled out because there is no evidence of lattice matching between the crystals of PBSU and PVDF. Transcrystallization is not a feasible mechanism for miscible polymer blends because of the size of domains. Thus, we consider that the oriented crystallization of PBSU is a result of confined crystallization of PBSU in the nanodomains of PBSU/PVDF blends. It has been reported that crystal orientation can be induced by spatial confinement of crystal growth.[31−33] Oriented crystallization in the confined state was first studied for polyethylene (PE)/polystyrene (PS) blends by Mencik et al.[31] They formed thin ribbonlike domains of PE in the melt-drawn samples of PE/PS blends. The crystal *b*-axis of PE was oriented parallel to the long dimensions of the ribbons because the *b*-axis is the axis of fastest crystal growth in the case of PE. In the case of the interlamellar exclusion structure, crystal growth of PBSU proceeds along the long axis of ribbonlike domains, which are oriented parallel to the flow direction. It was reported that the orientation of PBSU chains in the spherulites is quite similar to that of PE and that the chain axis is oriented in the tangential direction of the spherulites.[20] The molten chains of PBSU are also located in the narrow ribbonlike domains surrounded by the oriented lamellar morphologies of PVDF. As the diameter of the ribbonlike domains of PBSU is several tens of nanometers, crystal growth is confined along the flow direction, leading to the orientation of the growth axis parallel to the flow direction (Figures 6a and 7a). On the other hand, crystal growth of PBSU is confined to the planar domains between the lamellae of PBSU in the case of the interlamellar inclusion structure. The thickness of the planar domains is expected to be on the order of 10 nm. It was reported that the molecular chains are packed perpendicular to the basal plane of a thin single crystal of PBSU.[20] The crystal growth of PBSU proceeds parallel to the lamellar plane of PVDF, similar to the crystal growth in single crystals. Thus, the *b*-axis of PBSU is parallel to the lamellar plane of the interlamellar inclusion structure and the *c*-axis is normal to the lamellar plane (Figures 6b, 7b, and 10).

Conclusion

Oriented lamellar morphologies were formed in miscible PBSU/PVDF blends containing 30 wt % PBSU under uniaxial compression flow in the temperature range 140−163 °C. The lamellar structure is markedly affected by the processing temperature. The interlamellar exclusion structure is induced in films flow-oriented below 150 °C, whereas the interlamellar inclusion structure is stable in samples flow-oriented above 150 °C. The high degree of orientation is retained even when the processing temperature approaches the end-melting temperature of PVDF (161 °C). In this case, the oriented crystals of PVDF with high T_m are induced in the initial stage of compression processing, and those with normal T_m grow on the high-T_m crystals in the next step. Finally, the PBSU chains crystallize between the lamellae of PVDF, resulting in the formation of the interlamellar inclusion structure with a high degree of orientation. The interlamellar inclusion and interlamellar exclusion phenomena are explained by the formation and relaxation of tie molecules, which control the mutual diffusion of components in interlamellar regions.

The PBSU chains crystallize in the nanodomains of the PBSU/PVDF blends, resulting in the oriented crystallization of PBSU, which is correlated with the lamellar morphologies. The WAXD results indicate that the *b*-axis of PBSU crystals is oriented parallel to the flow direction and that the crystal *c*-axis is oriented perpendicular to the flow direction in samples with the interlamellar exclusion structure. On the other hand, the crystal *c*-axis of PBSU is preferentially oriented in the flow direction for samples having the interlamellar inclusion structure. Oriented crystallization of PBSU in the blends is explained by confined crystal growth, which forces the fastest growth axis of PBSU crystals to align parallel to the ribbonlike domains of the interlamellar exclusion structure and to the lamellar planes of the interlamellar inclusion structure.

Acknowledgment. This work was partially supported by a Grant-in-Aid for Scientific Research from the Japan Society for the Promotion of Science (JSPS). The authors are grateful to Dr. Tsuchihara of AIST for the measurements of molecular weights of samples.

References and Notes

(1) Khambatta, F. B.; Warner, F.; Russell, T.; Stein, R.S. *J. Polym. Sci., Part B: Polym. Phys.* **1976**, *14*, 1391.
(2) Silvestre, C.; Karasz, F. E.; MacKnight, W. J.; Martuscelli, E. *Eur. Polym. J.* **1987**, *23*, 745.
(3) Silvestre, C.; Cimmino, S.; Martuscelli, E.; Karasz, F. E.; MacKnight, W. J. *Polymer* **1987**, *28*, 1190.
(4) Cheung, Y. W.; Stein, R. S.; Lin, J. S.; Wignall, G. D. *Macromolecules* **1994**, *27*, 2520.
(5) Liu, L.-Z.; Chu, B.; Penning, J. P.; Manley, R. St. J. *Macromolecules* **1997**, *30*, 4398.
(6) Liu, L.-Z.; Chu, B.; Penning, J. P.; Manley, R. St. J. *J. Polym. Sci., Part B: Polym. Phys.* **2000**, *38*, 2296.
(7) Liu, J.; Jungnickel, B.-J. *J. Polym. Sci., Part B: Polym. Phys.* **2004**, *42*, 974.
(8) He, Y.; Zhu, B.; Kai, W.; Inoue, Y. *Macromolecules* **2004**, *37*, 3337.
(9) Terada, Y.; Ikehara, T.; Nishi, T. *Polym. J.* **2000**, *32*, 900.
(10) Hirano, S.; Terada, Y.; Ikehara, T.; Nishi, T. *Polym. J.* **2001**, *33*, 371.
(11) Ikehara, T.; Nishi, T. *Polym. J.* **2000**, *32*, 683−687.
(12) Zhao, Y.; Keroack, D.; Prud'homme, R. *Macromolecules* **1999**, *32*, 1218.
(13) Morin, D.; Zhao, Y.; Prud'homme, R. *J. Appl. Polym. Sci.* **2001**, *81*, 1683.
(14) Dikshit, A.; Kaito, A. *Polymer* **2003**, *44*, 6647.
(15) Park, J. W.; Doi, Y.; Iwata, T. *Macromolecules* **2005**, *38*, 2345.
(16) Li, Y.; Kaito, A.; Horiuchi, S. *Macromolecules* **2004**, *37*, 2119.
(17) Kaito, A. *Polymer* **2006**, *47*, 3548.
(18) Lee, J. C.; Tazawa, H.; Ikehara, T.; Nishi, T. *Polym. J.* **1998**, *30*, 327.
(19) Kaito, A. M.; Shimomura, M.; Akaba, M.; Nojima, S., submitted for publication in *J. Polym. Sci., Part B: Polym. Phys.*
(20) Ihn, K. J.; Yoo, E. S.; Im, S. S. *Macromolecules* **1995**, *28*, 2460.
(21) Trent, J. S.; Scheinbeim, J. I.; Couchman, P. R. *Macromolecules* **1983**, *16*, 589.
(22) Cakmak, M.; Teitge, A.; Zachamann, H. G.; White, J. L. *J. Polym. Sci., Part B: Polym. Phys.* **1993**, *31*, 371.
(23) Samon, J. M.; Schultz, J. M.; Hsio, B. S.; Seifert, S.; Stribeck, N.; Gurke, I.; Collins, G.; Saw, C. *Macromolecules* **1999**, *32*, 8121.
(24) Seth, K. K.; Kempster, C. J. E. *J. Polym. Sci., Polym. Symp.* **1977**, *58*, 297.
(25) Fornes, R. E.; Grady, P. L.; Hersh, S. P.; Bhat, G. R. *J. Polym. Sci., Part B: Polym. Phys.* **1976**, *14*, 559.
(26) Takahashi, T.; Inamura, M.; Tsujimoto, I. *J. Polym. Sci., Polym. Lett.* **1970**, *8*, 651.
(27) Nishio, Y.; Yamane, T.; Takahashi, T. *J. Macromol. Sci., Phys.* **1984**, *B23*, 17.
(28) Takahashi, T.; Nishio, Y.; Mizuno, H. *J. Appl. Polym. Sci.* **1987**, *34*, 2757.
(29) Li, Y.; Kaito, A. *Macromol. Rapid Commun.* **2003**, *24*, 255.
(30) Li, Y.; Kaito, A. *Polymer* **2003**, *44*, 8167.
(31) Mencik, Z.; Plummer, H. K.; Oene, H. V. *J. Polym. Sci., Part A-2* **1972**, *10*, 507.
(32) Schultz, J. M. *J. Polym. Sci., Part B: Polym. Phys.* **1992**, *30*, 785.
(33) Waddon, A. J.; Hill, M. J.; Keller, A.; Blundell, D. J. *J. Mater. Sci.* **1987**, *22*, 1773.

MA062952G